HAL open science

The onset of tapering in the early stage of growth of a nanowire

Saransh Raj Gosain, Edith Bellet-Amalric, Martien den Hertog, Régis André, Joël Cibert

To cite this version:

Saransh Raj Gosain, Edith Bellet-Amalric, Martien den Hertog, Régis André, Joël Cibert. The onset of tapering in the early stage of growth of a nanowire. Nanotechnology, 2022, 33 (25), pp.255601. 10.1088/1361-6528/ac5cfa . hal-03407728

HAL Id: hal-03407728

https://hal.science/hal-03407728v1

Submitted on 28 Oct 2021

HAL is a multi-disciplinary open access archive for the deposit and dissemination of scientific research documents, whether they are published or not. The documents may come from teaching and research institutions in France or abroad, or from public or private research centers.

L'archive ouverte pluridisciplinaire **HAL**, est destinée au dépôt et à la diffusion de documents scientifiques de niveau recherche, publiés ou non, émanant des établissements d'enseignement et de recherche français ou étrangers, des laboratoires publics ou privés.

The onset of tapering in the early stage of growth of a nanowire

Saransh Raj Gosain,[1] Edith Bellet-Amalric,[1] Martien den Hertog,[2] Régis André,[2] and Joël Cibert[2]
[1)] *Univ. Grenoble Alpes, CEA, Grenoble INP, IRIG, PHELIQS, Grenoble, France*
[2)] *Univ. Grenoble-Alpes, CNRS, Grenoble INP, Inst. NEEL, Grenoble, France*

(*joel.cibert@neel.cnrs.fr)

(Dated: 28 October 2021)

The early stage of growth of semiconductor nanowires is studied in the case where the sidewall adatoms have a short diffusion length due to a strong desorption. Experimental results are described for the growth of ZnSe nanowires by molecular beam epitaxy. They are discussed using the Burton-Cabrera-Frank description of the propagation of steps along the sidewalls, and compared to other II-VI and III-V nanowires. The role of the growth parameters and the resulting shape of the nanowires (cylinder, cone, or both combined) are highlighted.

PACS numbers: Valid PACS appear here

The final shape and final size of a nanowire must be tightly controlled as they are key parameters for the subsequent use of the nanowire. Typical shapes are schematized in Fig. 1a. While a pure cylinder shape appears most preferable for transport studies, a cone shape (tapered nanowire) allows a better extraction of the light from an embedded quantum dot[1–4], and the pencil shape, with a long thick cylinder and a strong tapering isolated near the nanowire tip[5] ("P" in Fig. 1a) may be preferable for a better light collection in photovoltaic devices[6,7]. Similar shapes and sizes have been demonstrated for different systems in spite of large differences in the material parameters, for instance ZnTe and InP with orders of magnitudes difference in the diffusion length along the nanowire[8]. However, the growth strategy has to be adapted to each material and the range of available values of length and radius has to be determined.

Models have been proposed for the initial nucleation and the transformation into nanowires[9–11]. In the stage of growth following this nucleation, whether and how tapering appears strongly depends on the material involved and on the growth conditions. The pencil-shape of III-V nanowires[12] has attracted a lot of attention from theoreticians. The most precise description of the radial growth involves the nucleation and propagation of atomic steps along the nanowire sidewalls[13,14]. The pencil shape ("P" in Fig. 1a) is obtained when an initial cylinder broadens while keeping the cylinder-shape, as the steps on the sidewalls propagate up to the seed droplet, and remain stuck there by the depletion of adatoms. Tapering is expected to occur when the nanowire length exceeds the sidewall diffusion length. By contrast, II-VI nanowires start with a cylinder-shape with a constant radius (determined by the seed radius, shape "C" in Fig. 1a)[15], and then develop a cone shape[16] while keeping the cylinder segment on top of the cone ("CC" in Fig. 1a), as the sidewall steps do not reach the seed[8].

The goal of the present study is to describe more precisely the early stage of the growth of II-VI nanowires. We give experimental results obtained for short ZnSe nanowires. Then, we emphasize the key points of the models we use to describe the growth of II-VI nanowires by gold-seeded molecular beam epitaxy (MBE). And finally, we compare the experimental results with the calculated profiles of the adatom density along the sidewalls.

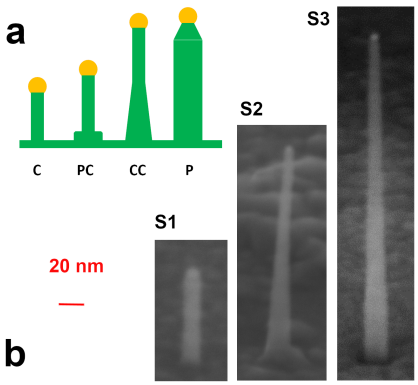

FIG. 1. (a) Schematics of characteristic nanowire shapes (C-cylinder, PC=cylinder on pedestal, CC=cylinder on cone, P=pencil). (b) SEM images at 65° of ZnSe nanowires from sample S1, sample S2, and sample S3 as indicated. All images with the same scale bars at 20 nm.

ZnSe nanowires were grown on (111)B ZnSe buffer layers on top of (111)B GaAs substrates, using solid gold nanoparticles as seeds (the so-called Vapor-Solid-Solid, or VSS, growth mode). The growth conditions (beam from standard Zn and Se Knudsen cells, moderate Se excess of the order of a factor 2 (in atom $cm^{-2}s^{-1}$), substrate at 350°C[17,18]) lead to micrometer long nanowires for a growth time around 1 h, with a small-angle tapering visible over the whole nanowire length. A series of twelve nanowire samples were grown under these conditions, with a nanowire length up to 2.5 μm. It includes eight samples below 400 nm. Hereafter we focus onto these shorter nanowires.

Figure 1b displays Scanning Electron Microscopy (SEM) images of three characteristic samples. The growth time was 8 min for sample S1, 20 min for S2, and 32 min for S3, resulting in an average length of 110 ± 15 nm, 230 ± 20 nm, and 380 ± 20 nm, respectively, from statistics over SEM images such as in Fig. 1. Based on these SEM observations, and on complementary observations at different values of the nanowire length over the whole series of samples, we identify

three growth stages, each of them featuring a characteristic shape:

- very short nanowires, with a length $L < 150$ nm, are cylindrical, with a radius in the order of the nanoparticle radius, as exemplified in Fig. 1b, S1. The radius is too small to be accurately measured by SEM due to the presence of an amorphous layer which covers the nanowire and the nanoparticle. From Transmission Electron Microscopy (TEM) images of nanowires (Fig. 2a) from the same sample S1 as Fig. 1, the radius of the nanoparticle $R_{NP} = 3$ to 5 nm and the radius of the nanowire R_{NW} is smaller by typically ~ 0.5 nm (see the radial profile of one nanowire in Fig.2a). Tridimensional objects progressively appear on the surface between the nanowires, as well as pedestals at the base of the nanowires.

- intermediate nanowires, with L between 150 and 300 nm, exhibit a clear cone at their base, as exemplified in Fig. 1b, sample S2. The radius of this cone is in the order of the radius of the pedestal of short nanowires, and its length progressively increases as L increases. For the nanowire of Fig. 2b, the cone half-angle $\theta = 0.04$ rad and the length of the cylinder ~ 80 nm. The transition from the cone to the cylinder may be well-defined, such as in the plot of the radius *vs.* position in Fig. 2b, or more progressive.

- long nanowires, with $L > 300$ nm, exhibit (Fig. 1b, sample S3) a ~ 100 nm long cylinder at the tip, on top of a cone section with a length which increases with L, as exemplified in Fig. 1b. The tapering angle in the cone section remains fairly constant as L increases up to the μm range (half-angle $\theta = 0.01$ rad under the present growth conditions), so that the base radius increases with L. The base itself is hidden by a 2D layer resulting from the coalescence of the previous 3D objects. More details are given in Ref. 17 and 18.

We now briefly summarize the main features of the diffusion-limited model of nanowire growth which has been previously applied to describe the shape of long ZnTe nanowires[8,16], with a focus on the results which are relevant for the present study.

The flux impinges the substrate, nanowire and gold nanoparticle, at an angle α with respect to the normal to the substrate, which is also the nanowire axis. In the present case, we have checked that the flux which governs the axial and radial growth rates is that of Zn atoms[17,18]: In our MBE chamber, the position of the Zn cell is such that $\tan\alpha = 0.78$. The flux F is calibrated from the growth rate $F\cos\alpha$ of a ZnTe layer under an excess of Te, for which complete sticking is assumed. In the following, the flux and the growth rates are expressed in nm per unit time. The adatom density is expressed in nm, as the number of adatoms per unit area multiplied by the thickness of a ZnSe monolayer. With this conventions, these quantities are independent of the crystal orientation.

The main contribution to the nanowire growth is from diffusion of adatoms along the sidewalls towards the nanoparticle[19,20]. The flux to the nanowire sidewalls, $F\sin\alpha$, is intercepted by the nanowire diameter, $2R_{NW}$, and distributed over the perimeter $2\pi R_{NW}$; Hence the average flux is $F_\alpha = F\frac{\sin\alpha}{\pi}$. Far from both ends of a long nanowire, the adatom density is $n = F_\alpha\tau$, where τ is the residence time of the adatoms.

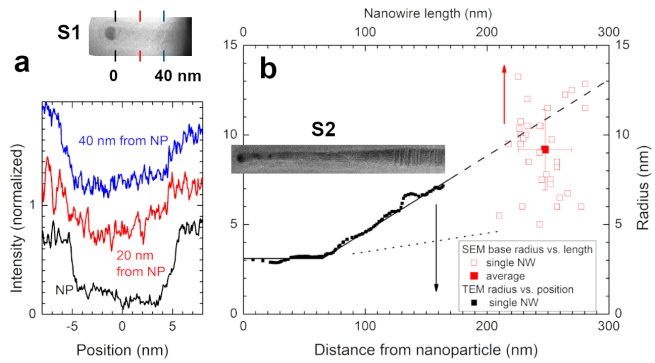

FIG. 2. TEM images of nanowires, and profiles. In these TEM images, the base of the nanowire is masked by the edge of the cleaved substrate. Panel (a) shows the image of a nanowire from sample S1, and radial intensity profiles, at three positions along the axis, as indicated; Panel (b) shows a nanowire from sample S2, in front of the plot of the radius *vs.* position of the same nanowire. Black closed squares are experimental data and the dashed lines show the linear fit. The base radius *vs.* the nanowire length, measured by SEM on a series of nanowires from the same sample S2, is shown by open red squares. The closed red square gives the average value and standard deviation. The dotted line shows the tapering of long nanowires. Same scale for the image and the plot.

The diffusion along the nanowire is described by a diffusion coefficient D. In a simple approximation, the adatom density at distance z from the base of the nanowire is calculated assuming that the nanoparticle acts as a perfect trap at the top of the nanowire: The boundary condition is $n(z = L) = 0$. This assumption was found to describe adequately the growth of ZnTe nanowires[16]. The boundary condition at the base of the nanowire, $z = 0$, depends on the configuration of the nanowire-substrate interface. An easy transfer of adatoms between the substrate surface and the nanowire sidewall results in a condition of equal currents on both sides[16,20]. This may be the case here for the very early stage of the nanowire growth. However, we have observed the rapid formation of a pedestal at the base of the nanowire: This pedestal likely stops the transfer of adatoms from the substrate to the nanowire, and again the boundary condition should be that of a perfect trap, $n(z = 0) = 0$.

With both boundary conditions, the adatom density is

$$n(z) = F_\alpha\tau\left[1 - \frac{\cosh\frac{\frac{L}{2}-z}{\lambda}}{\cosh\frac{L}{2\lambda}}\right], \qquad (1)$$

where $\lambda = \sqrt{D\tau}$ is the diffusion length on the sidewall.

Figure 3a shows three examples of adatom density profiles, for a short nanowire ($L = 3\lambda$), an intermediate one ($L = 8\lambda$)

and a long one ($L = 30\lambda$). These profiles will be discussed later on.

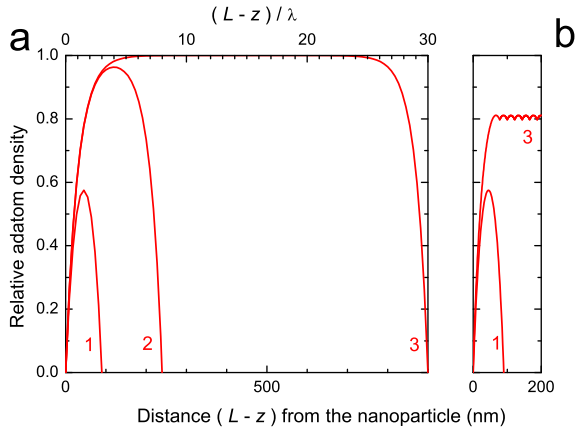

FIG. 3. (a) Adatom density divided by $F_\alpha \tau$ (flux $\times$ residence time), for three nanowires with length L equal to (1) 3λ, (2) 8λ and 30λ, where λ is the diffusion length (top scale). With $\lambda = 30$ nm, the respective lengths are 90 nm, 240 nm and (3) 900 nm (bottom scale). (b) Same as (a), taking into account the incorporation at step edges (Burton-Cabrera-Frank model[8,13,14]).

This model is a reasonable approximation to describe the axial growth rate of the nanowire. The current of adatoms ($-D\frac{dn}{dz}$) towards the nanoparticle, through the perimeter $2\pi R_{NW}$, contributes to the axial growth of the nanowire, by the formation of monolayers of area πR_{NW}^2. For a long nanowire ($L \gg \lambda$), the current at the nanowire tip is $-\lambda F_\alpha$ and we obtain

$$\frac{dL}{dt} = F_\alpha \frac{2\lambda}{R_{NW}} + \kappa F. \qquad (2)$$

The second term is the contribution from the direct flux to the nanoparticle. The prefactor κ is a function of the nanoparticle or nanodroplet shape, the interface with the nanowire tip, and the angle of incidence α[8,21]. From the TEM images of the nanoparticle (Fig. 2), we estimate $\kappa = 1.6$ and $R = 4$ nm. If we further assume that the radial growth rate is proportional to the local adatom density, we expect a constant radial growth (hence the formation of a regular cone) for the central part of the long nanowires where the adatom density is constant, $n = F_\alpha \tau$. We also expect a reduced radial growth rate at the tip and for short nanowires.

The exact shape of the nanowire, including in the vicinity of the tip, can be analyzed more accurately by calculating the propagation of steps along the nanowire sidewall, in a Burton-Cabrera-Frank approach[13,14]. A steady state configuration is realized[8] by a succession of terraces of length $2l_s$ separated by steps of height a (the monolayer thickness), with a cylinder of length $(l_0 + l_s)$ at the tip. This is the configuration labelled CC in Fig. 1a. Adatoms diffuse on the terraces with a probability $p_{des} = \frac{1}{\tau}$ to desorb, thus defining a diffusion length λ. The incorporation takes place not only at the nanowire tip through the nanoparticle, but also at the steps, with a finite probability p_{inc}. The step velocity is governed by the terrace length (the step-step distance), while the nanowire axial growth rate is governed by the tip cylinder length and the value of κ. The steady-state condition imposes that the step velocity matches the nanowire axial growth rate. Therefore a steady state imposes a relationship between the terrace length and the tip cylinder length, given by Eq. 5 of Ref. [8].

The material parameters are λ_{des}, and p_{inc}/p_{hop}, where p_{hop} is the hopping probability to the nearest site on the terrace. Their value is determined by fitting the characteristics of long nanowires (such as the nanowire in Fig. 1b and longer ones[17,18]). We obtain $\lambda = 30$ nm and $p_{inc}/p_{hop} = 10^{-3}$. The corresponding adatom density profile is shown by curve (3) in Fig. 3b. Each kink corresponds to a step, and the step velocity is proportional to the adatom density at this position.

We show now that the three examples in Fig. 3 well match the three shapes identified in Fig. 1.

For the long nanowires, the Burton-Cabrera-Frank model describes a growth with a constant tapering angle. The cone increases in length and radius, and it is terminated at the tip by a cylinder of constant length. With the parameters given previously, we calculate a cylinder length ~ 80 nm.

Turning now to the shortest nanowire (#1 in Fig. 3), the adatom density is small, implying that the step velocity remains much lower than the nanowire growth rate: This corresponds to the growth of a thin cylinder, with a diameter matching the contact with the nanoparticle, as observed in Fig. 1a and Fig. 2a. Note that we have no evidence that the pedestal forms before the NWs start to grow, as described in Ref.[22]: In the absence of such a trap, adatoms may diffuse from the substrate to the NW sidewall, and speed up the axial growth until the pedestal is in place and constitutes a trap.

As the adatom density increases, the velocity of steps increases, so that the velocity of the leading step can reach the nanowire growth rate (thus inducing a stabilized cylinder length) for a nanowire such as #2. Steps behind the leading ones (closer to the nanowire base) see a smaller adatom density, which means that the velocity of these steps is smaller. The result is a tapered profile below the tip cylinder, with an angle larger than the steady-state value of nanowire #3 but decreasing as growth proceeds. In the absence of an analytical solution such as available for the long nanowires[8], determining the exact shape of the nanowire in this case calls for a numerical solution of the whole profile. Note however that the length of the cylinder observed in Fig. 2b nicely agrees with the length ~ 80 nm predicted by the Burton-Cabrera-Frank model for long nanowires.

Finally, the steady-state cone increases in length as more and more steps reach the steady-state velocity.

Hence the characteristic shapes identified in Fig. 1 match the characteristic profiles of the adatom density in Fig. 3, calculated with the material parameters deduced from the properties of the long nanowires.

The value of λ means that the desorption of adatoms from the ZnSe sidewalls is strong. It is even stronger than for ZnTe nanowires with the zinc-blende structure, where λ=90 nm[8]. Much larger values of the diffusion length are commonly reported for III-V nanowires, for instance $\lambda \simeq 1$ μm for InP

nanowires[8]. We observe nevertheless a significant radial growth, and tapered nanowires can be grown. These ZnSe nanowires with the wurtzite structure thus appear intermediate between the wurtzite ZnTe nanowires which maintain a cylinder shape whatever their length[16], and zinc-blende ZnTe nanowires or InP nanowires, for which the incorporation is large enough that it impacts or even limits the axial growth[8].

Similar features were observed in the early stage of growth of zinc-blende ZnTe nanowires[15], with a smaller desorption and a stronger sticking: Nanowires with $L = 140 \pm 60$ nm are still mainly cylinder-shaped.

Our intermediate shape make a contrast with the pencil-like shape nanowires made of III-V semiconductors such as InP[23], InAs[12] or GaAs[5]. This remarkable shape was modelled assuming no desorption of adatoms[13,14]. It is considered experimentally to be characterized by a long diffusion length along the nanowire sidewall, even if the radial growth starts with a delay with respect to the axial growth[24]. However, InP nanowires grown by Metal-Organic MBE exhibit a significant lateral growth[25–27], which gives rise directly to the cone+cylinder shape and not to the pencil-like shape. These nanowires can be described with an easy attachment to the step edge[8] so that the diffusion along the nanowire sidewall is limited by incorporation while the desorption diffusion length is in the micrometer range. The MBE growth of ZnSe and ZnTe nanowires is characterized by a progressive change of shape as growth proceeds: from a thin cylinder, to a thin cylinder on top of an open cone, and finally a thin cylinder on top of a long cone with a small, steady-state angle. This sequence appears to be correlated with the profile of the adatom density along the sidewalls, and hence to be governed by the ratio of the nanowire length to the diffusion length, which is mostly determined by the desorption of adatoms from the nanowire sidewalls.

To conclude, we identify experimentally two stages of growth of ZnSe nanowires before they reach a steady-state shape with a constant tapering angle. Very short nanowires are cylinder-shaped with no radial growth. Nanowires of intermediate length comprise a cylinder section on top of a cone section, with a tapering angle which progressively decreases to the steady-state value. There three shapes, and their boundaries, are well accounted for using a Burton-Cabrera-Frank model with a strong desorption of the adatoms from the sidewalls.

Acknowledgements. SRG acknowledges the European Union's Horizon 2020 research and innovation programme under the Marie Skłodowska-Curie grant agreement No 754303 (GREnoble QUantum Engineering), and we gratefully thank Kuntheak Kheng for numerous discussions.

[1] J. Claudon, N. Gregersen, P. Lalanne, and J.-M. Gérard, Harnessing Light with Photonic Nanowires: Fundamentals and Applications to Quantum Optics ChemPhysChem **14**, 2393 (2013).

[2] I. E. Zadeh, A. W. Elshaari, K. D. Jöns, A. Fognini, D. Dalacu, P. J. Poole, M. E. Reimer, and V. Zwiller, Deterministic Integration of Single Photon Sources in Silicon Based Photonic Circuits Nano Lett. **16**, 2289 (2017).

[3] A. W. Elshaari, I. E. Zadeh, A. Fognini, M. E. Reimer, D. Dalacu, P. J. Poole, V. Zwiller, and K. D. Jöns, On-chip single photon filtering and multiplexing in hybrid quantum photonic circuits, Nature Comm. **8**, 379 (2017).

[4] D. Dalacu, P. J. Poole, and R. L. Williams, Tailoring the Geometry of Bottom-Up Nanowires: Application to High Efficiency Single Photon Sources, Nanomaterials **11**, 1201 (2021).

[5] M. C. Plante and R. R. LaPierre, Au-assisted growth of GaAs nanowires by gas source molecular beam epitaxy: Tapering, sidewall faceting and crystal structure, J. Crystal Growth **310**, 356 (2008).

[6] Yingfeng Li, Meicheng Li, Pengfei Fu, Ruike Li, Dandan Song, Chao Shen, and Yan Zhao, A comparison of light-harvesting performance of silicon nanocones and nanowires for radial-junction solar cells, Scientific Reports **5**, 11532 (2015).

[7] Wipakorn Jevasuwan, Junyi Chen, Thiyagu Subramani, Ken C. Pradel, Toshiaki Takei, Kotaro Dai, Kei Shinotsuka, Yoshihisa Hatta and Naoki Fukata, Pencil-shaped silicon nanowire synthesis and photovoltaic application, Japanese J. Appl. Phys. **56**, 085201 (2017).

[8] E. Bellet-Amalric, R. André, C. Bougerol, M. den Hertog, A. Jaffal, and J. Cibert, Controlling the shape of a tapered nanowire: lessons from the Burton-Cabrera-Frank model, Nanotechnology **31**, 274004 (2020).

[9] N. V. Sibirev, M. B. Nazarenko, G. E. Cirlin, Y. B. Samsonenko, and V. G. Dubrovskii, The initial stage of growth of crystalline nanowhiskers, Semiconductors **44**, 112 (2010).

[10] S. N. Filimonov and Y. Y. Hervieu, Kinetic Model of the Initial Stage of the Nanowire Growth, Russian Phys. J. **60**, 2040 (2018).

[11] Y. Y. Hervieu, On the kinetics of the early stage of growth of III-V nanowires, J. Cryst. Growth **568**, 126187 (2021).

[12] M. Tchernycheva, L. Travers, G. Patriarche, F. Glas, J. -C. Harmand, G. E. Cirlin, and V. G. Dubrovskii, Au-assisted molecular beam epitaxy of InAs nanowires: Growth and theoretical analysis, J. Appl. Phys. **102** 094313 (2007).

[13] S. N. Filimonov and Y. Y. Hervieu, Model of step propagation and step bunching at the sidewalls of nanowires, J. Cryst. Growth **427**, 60 (2015).

[14] S. N. Filimonov and Y. Y. Hervieu, Step Flow Model of Radial Growth and Shape Evolution of Semiconductor Nanowires, Russ. Phys. J. **59**, 1206 (2016).

[15] P. Rueda-Fonseca, PhD thesis Université Grenoble-Alpes, 2015.

[16] P. Rueda-Fonseca, M. Orrù, E. Bellet-Amalric, E. Robin, M. Den Hertog, Y. Genuist, R. André, S. Tatarenko, and J. Cibert, Diffusion-driven growth of nanowires by low-temperature molecular beam epitaxy, J. Appl. Phys. **119**, 164303 (2016).

[17] S. R. Gosain, PhD thesis, Université Grenoble-Alpes, 2021.

[18] S. R. Gosain, *et al.*, MBE growth of ZnSe nanowires and core-shell nanowires.

[19] V. Ruth and J. P. Hirth, Kinetics of Diffusion Controlled Whisker Growth, J. Chem. Phys. **41**, 3139 (1964).

[20] V. G. Dubrovskii, N. V. Sibirev, R. A. Suris, G. E. Cirlin, V. M. Ustinov, M. Tchernysheva, and J. C. Harmand, The role of surface diffusion of adatoms in the formation of nanowire crystals, Semiconductors **40**, 1075 (2006).

[21] F. Glas, Vapor fluxes on the apical droplet during nanowire growth by molecular beam epitaxy, Phys. Status Solidi B **247**, 254 (2010).

[22] S. N. Filimonov and Y. Y. Hervieu, Kinetics of Step Propagation at the Sidewalls of 3D Islands and Nanowires, e-J. Surf. Sci. Nanotech. **12**, 68 (2014).

[23] A. Jaffal, W. Redjem, P. Regreny, Hai-Son Nguyen, S. Cueff, X. Letartre, G. Patriarche, E. Rousseau, G. Cassabois, M. Gendry, and N. Chauvin, InAs quantum dot in a needlelike tapered InP nanowire: a telecom band single photon source monolithically grown on silicon, Nanoscale **11**, 21847 (2019).

[24] V. G. Dubrovskii, Reconsideration of Nanowire Growth Theory at Low Temperatures, Nanomaterials **11**, 2378 (2021).

[25] Y. Greenberg, A. Kelrich, Y. Calahorra, S. Cohen, and D. Ritter, Tapering and crystal structure of indium phosphide nanowires grown by selective area vapor liquid solid epitaxy, J. Crystal Growth **389**, 103 (2014).

[26] A. Kelrich, V. G. Dubrovskii, Y. Calahorra, S. Cohen, and D. Ritter, Control of morphology and crystal purity of InP nanowires by variation of phosphine flux during selective area MOMBE, Nanotechnology **26**, 085303 (2015).

[27] V. G. Dubrovskii, M. A. Timofeeva, A. Kelrich, and D. Ritter, Growth and morphological modeling of InP nanowires obtained by Au-catalyzed selective area MOMBE, J. Cryst. Growth **413**, 25 (2015).